Dynamic Scaling of the Cluster-Size Distribution in Nucleation: Precoalescence Stages

Frank G. Shi
Biochemical Engineering/Materials Science & Engineering Programs,
School of Engineering, University of California, Irvine, CA 92717

John H. Seinfeld
Dept. of Chemical Engineering, California Institute of Technology, Pasadena, CA 91125

The dynamic evolution of the cluster-size distribution (CSD) in the precoalescence stages of nucleation and growth for sizes within and beyond the nucleation barrier layer (NBL) has been obtained. The existence of several universal kinetic laws of nucleation is predicted. In the precoalescence stages of nucleation, the CSD for sizes within and beyond the NBL obeys dynamic scaling relations. In a range of sizes beyond the NBL, the CSD exhibits a universal power law behavior, the exponent of which depends only on the interphase monomer transfer mechanism. Based on the results for the CSD, a general foundation is developed for nucleation kinetic measurements including the determination of the nucleation barrier and the interfacial monomer transport rate by measuring the CSD. A preliminary comparison with an experimental study confirms the predicted dynamic scaling and the power law behavior of the CSD in the early stages of nucleation and growth.

Introduction

As observed recently by Kelton (1992), even the most common microscopic models embodied in nucleation theories have not been explicitly verified or disproved experimentally. A present challenge is to develop a general foundation for kinetic measurements that can be used for designing experiments and analyzing data to elucidate fundamental mechanisms. Such a foundation, as will be discussed, can be based on observations of the cluster-size distribution (CSD) in the early stages of nucleation and growth. The essential features of the nucleation process are embodied in the cluster-size distribution for sizes in the nucleation barrier layer (NBL) and beyond (Shi and Seinfeld, 1992). The transient evolution of the CSD for sizes in the NBL has been obtained for uninary (Shi et al., 1990) and for binary nucleation (Shi and Seinfeld, 1990). However, the question of how to treat the CSD for sizes beyond the NBL has defied analytic solution from early attempts (Feder et al., 1966) up to the present (Russell, 1980; Shi et al., 1990). The transient solutions can be applied rigorously to nucleation in solids without requiring long-range transport (Tu et al., 1992); however, in general, the dynamic effect due to the depletion of the monomer density because of nucleation and growth has to be addressed.

It is the purpose of this article to study the dynamic scaling behavior of the CSD for sizes within and beyond the NBL and other kinetic laws during the early stages of nucleation. The results afford a systematic method to test various microscopic models involved in nucleation theories by measuring the CSD for sizes beyond the NBL in the precoalescence stages.

Kinetic Description

For phase transformations initiated by nucleation, a subcritical cluster-size distribution has to be formed preceding the appearance of nuclei of the new phase. The growth and shrinkage of those clusters are usually dominated by addition or removal of single monomers. If the addition rate of single monomers to a cluster consisting of g monomers is denoted as $\beta(g, t)$, then the dissociation rate of single monomers from the same cluster can be determined from $\beta(g, t)$ and the formation energy of a g-sized cluster, $W(g)$. Nucleation is char-

acterized by $W_* \gg kT$, where W_* denotes the maximum of $W(g)$. Then, the cluster number concentration, $f(g, t)$, can be described by the following kinetic equation (Frenkel, 1946):

$$\frac{\partial f(g, t)}{\partial t} = \frac{\partial}{\partial g}\left[\beta(g, t)\frac{\partial f(g, t)}{\partial g} - \dot{g}_m f(g, t)\right],$$

$$\dot{g}_m = -\frac{\beta(g, t)}{kT}\frac{\partial W(g)}{\partial g}. \quad (1)$$

In this work, the term cluster-size distribution is used equivalently to the cluster number concentration as a function of size. As a continuous equation, Eq. 1 is accurate enough for g down to about 10 (Frenkel, 1946). A refining of Eq. 1 does not alter any universal kinetic behavior of nucleation, as will be confirmed by this work.

It is not necessary to know the exact functional form of $W(g)/kT$ to solve Eq. 1 for $f(g, t)$; the universal kinetic laws of nucleation depend on the value of $W(g)/kT$, but not its particular functional form with respect to g, as will be revealed by this work. Therefore, for the purpose of illustration, one may first simply consider the following form (Mon and Jasnow, 1987):

$$W(g) = -g\Delta\mu + s\sigma g^{(d-1)/d}, \quad (2)$$

where $\Delta\mu$ is the nucleation driving force, $\theta = s\sigma/kT$, σ is the interfacial free energy per unit "area" between the bulk phases, s is a geometrical constant, k is Boltzmann's constant, T is temperature and d is the effective dimensionality of the cluster.

The size dependence for most mechanisms of monomer addition to clusters (Zettlemoyer, 1969; Russell, 1980) can be included within the form:

$$\beta(g, t) \propto n_c(t) g^{(d-\nu)/d}. \quad (3)$$

where ν is an index that governs different modes of monomer addition, and $n_c(t)$ is the interfacial monomer concentration around the cluster. For cluster formation controlled by the formation of a chemical bond between the monomer and the cluster of $d=3$, $\nu=1$, hence, $\beta(g) \propto g^{2/3}$. If nucleation of compact clusters is controlled by the diffusion of single monomers to the cluster of $d=3$, $\nu=2$, then $\beta(g) \propto g^{1/3}$. For concreteness, $d=3$ shall be considered: $\nu=1$, $\beta(g) \propto g^{2/3}$. In general, $n_c(t) = n(1, t)$.

Considering an abrupt change in supersaturation of the system from $t=0$ to $t=0^+$, the system can be taken as initially cluster-free:

$$f(g>1, 0) = 0. \quad (4)$$

Since the formation of clusters takes place for $g \geq 1$, there is no flux in the size space for $g=1$. Therefore,

$$\lim_{g\to 1} f(g, t)/n(g, t) \to f(1, t)/n(1, t) \to 1. \quad (5)$$

where

$$n(g, t) = n(1, t)\exp[-W(g)/kT]. \quad (6)$$

is a metastable equilibrium cluster distribution for $g \leq g_o$ under the supersaturation conditions. Here, g_o is the size corresponding to a so-called nucleated cluster that is sufficiently larger than the critical cluster (Shi and Seinfeld, 1991, 1992), and $n(1, t)$ is the available monomer number concentration of the nucleating system under consideration at time t. Nucleation does not occur instantaneously after an abrupt change in supersaturation, because the subcritical and critical cluster-size distributions have to develop. The finite time required in forming the subcritical and critical cluster-size distributions indicates that the supersaturated system can be treated as metastable. As a consequence, Eq. 6 can be introduced.

The monomer number density, $n(1, t)$, depends on time because of the depletion of the monomer due to the incorporation of the monomers into the nucleating and growing clusters. Usually,

$$n(1, t) \approx n(1, 0)[1 - \alpha(t)],$$

where $\alpha(t)$ is the volume fraction of the nucleated phase at time t. It is within experimental capability to determine $\alpha(t)$ and thus $n(1, t)$ during nucleation and growth; $n(1, t)$ can be taken as a known quantity.

We will study the dynamic evolution of the CSD by seeking analytic solutions to the system of Eqs. 1 to 5 under the conditions of time-independent temperature, pressure and $W(g)$ for $t>0$. An example of such a situation is nucleation in amorphous solids under isothermal annealing (Tu et al., 1992). The approaches developed for obtaining the CSD are sufficiently general to consider situations corresponding to different initial and boundary conditions.

CSD within the Nucleation Barrier Layer

Nucleation barrier layer

One of the most important characteristics of nucleation is the existence of the subcritical, critical and supercritical regions. The critical region or the nucleation barrier layer is defined as the region in which (Feder et al., 1966):

$$|W(g) - W_*| \leq kT. \quad (7)$$

If the critical cluster-size corresponding to the maximum of $W(g)$ is g_*, the width of the NBL 2δ is:

$$\delta = \left[-\frac{1}{2kT}\frac{\partial^2 W}{\partial g^2}\right]^{-1/2}\Bigg|_{g=g_*} = 3g_*^{2/3}\theta^{-1/2} \quad (8)$$

which is related to the Zeldovich factor Z by $\delta = 1/\sqrt{\pi}Z$. Hence, the NBL is the region defined by $g_* - \delta < g < g_* + \delta$. The subcritical and supercritical regions are to the right and left of the NBL, respectively: $g > g_* + \delta$ and $g < g_* + \delta$, as sketched in Figure 1.

Approach

The existence of the critical, subcritical and supercritical regions determines that the system of Eqs. 1 to 5 cannot be

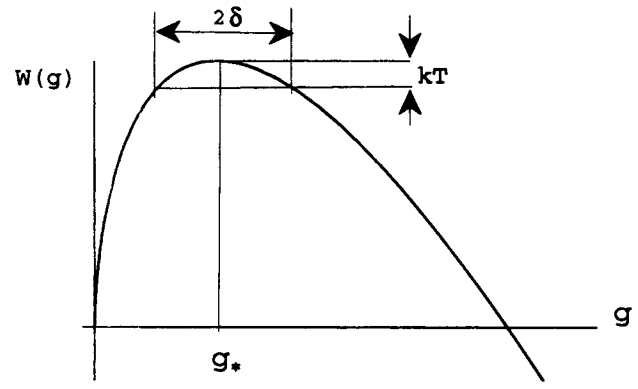

Figure 1. Nucleation barrier layer whose thickness is 2δ.

solved at once to obtain an expression for $f(g, t)$ that is valid uniformly over all sizes. Nevertheless, the existence of the critical region or the nucleation barrier layer provides the exact basis for employing boundary layer theory to deal with the present problem (Bender and Orszag, 1978) to study the dynamic evolution of the CSD in nucleation (Shi et al., 1990).

Considering $d=3$, $\nu=1$ and introducing

$$\delta/g_* \equiv \epsilon, \quad x=g/g_*, \quad y(x, t)=f(x, t)/n(x, t), \tag{9}$$

into Eq. 1, we have:

$$x^{-2/3}\tau\left[\frac{\partial y(x, t)}{\partial t}+y(x, t)\frac{\partial \ln n(x, t)}{\partial t}\right] = \frac{1}{2}\epsilon^2\frac{\partial^2 y(x, t)}{\partial x^2}+\left[\frac{1}{3x}\epsilon^2+3(1-x^{-1/3})\right]\frac{\partial y(x, t)}{\partial x} \tag{10}$$

where

$$\tau(t)=\delta^2/2\beta(g_*, t) \quad \beta_*(t)\equiv\beta(g_*, t)\propto n_c. \tag{11}$$

We will first solve Eq. 10 to obtain the CSD under the condition of $|\partial y(x, t)/\partial t| \gg |y(x, t)\partial \ln n(x, t)/\partial t|$. Then, the approach developed previously (Shi et al., 1990) can be followed.

Since $\epsilon=\sqrt{3kT/W_*}\ll 1$ for $W_* \gg kT$, Eq. 10 can be reduced to a first-order equation in the right and left regions. The left outer solution can be obtained with the left outer boundary condition, Eq. 5. The right outer solution, however, is not known beforehand, and, in fact, it is our ultimate goal to obtain $f(g, t)$ valid in the region of $g/g_*>1+\epsilon$. Since $n(g, t)$ becomes exponentially large for $g \gg g_*+\delta$, while $f(g, t)$ is finite, one has:

$$f(g, t)/n(g, t)\to 0, \quad g/g_* \gg 1. \tag{12}$$

Equation 12 is of importance in that it replaces the traditionally used boundary condition, $f(g\to\infty, t)=0$.

As expected, the outer solutions are not valid near $x=1$, and there is a transition boundary layer about $x=1$. Since the thickness of this boundary layer is found to be ϵ, the inner variable $X=(x-1)/\epsilon$ should be introduced (Shi et al., 1990). In terms of the inner variable, Eq. 1 can be simplified in the NBL as (Shi et al., 1990):

$$\tau\frac{\partial y(X, t)}{\partial t}=\frac{1}{2}\frac{\partial^2 y(X, t)}{\partial X^2}+X\frac{\partial y(X, t)}{\partial X} \tag{13}$$

Two unknown constants in the inner solution to Eq. 13 valid for the NBL can be determined by matching the inner solution with the two outer solutions.

The necessary right outer solution is determined by Eq. 12. The right outer solution is:

$$f(g, t)/n(g, t)=0$$

which does not imply that $f(g, t)=0$, but states the fact that $f(g, t)/n(g, t)$ is exponentially small (Shi et al., 1991; Shi and Seinfeld, 1992). Both the right and left outer solutions obtained in terms of $f(g, t)/n(g, t)$ are used for the *sole* purpose of determining $f(g, t)$ within the NBL. Moreover, as mentioned above, $n(g, t)$ is well defined only for $g\le g_o\approx g_*+1.1\delta$. For $g>g_o$, however, $n(g, t)$ is physically meaningless. Thus, the right outer solution $f(g, t)/n(g, t)=0$ is not the actual CSD for $g>g_o$. That is the most essential point of our approach based on boundary layer theory.

Dynamic scaling of the CSD within the NBL

With the initial and boundary conditions given by Eqs. 4 and 5, respectively, Eq. 10 can be solved by following the approach outlined above to obtain, for $g_*-\delta<g<g_*+\delta$:

$$f(g, t)/n(g, t)=\frac{1}{2}\text{erfc}\left[\frac{g-g_*}{\delta}+\exp\left(-\frac{t-\lambda\tau}{\tau}\right)\right] -\frac{1}{2}\text{erfc}\left[\frac{g-g_*}{\delta}+e^{\lambda}\right], \tag{14}$$

where

$$\lambda=g_*^{-1/3}-1+\ln(1-g_*^{-1/3})+\frac{1}{2}\ln\frac{3W(g_*)}{kT} = -\frac{1}{\tau}\int_1^{g_*-\delta}\frac{dg}{g_m}=\lim_{g\to g_*-\delta}\mu(g). \tag{15}$$

For $g_* \gg 1$, Eq. 14 gives $\lambda=-1+1/2\ln(3W_*/kT)$. In our previous work on transient nucleation (Shi et al., 1990, 1991; Shi and Seinfeld, 1990, 1991, 1992), the second term on the righthand side of Eq. 14 was unfortunately neglected. As a result, there is a discrepancy between our previous result for $y_{in}(x, t=0)$ and the initial condition, Eq. 4. This important issue has been solved, and Eq. 14 is free of the discontinuity problem. The detailed mathematical procedural will be presented elsewhere (Shi and Seinfeld, 1993).

The dynamic evolution of $f(g, t)/n(1, t)$ according to Eq. 14 is shown in Figure 2.

The dynamic evolution of $f(g, t)/n(1, t)$ in the NBL revealed by Eq. 14 is apparently universal, since a particular $W(g)$

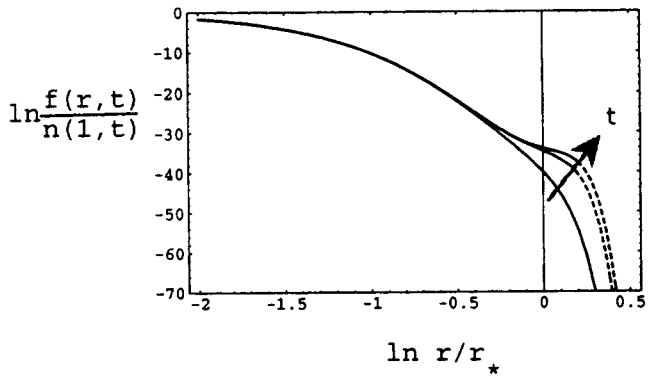

Figure 2. Dynamic evolution of the CSD for sizes within the NBL for $t/\tau = 0.5, 2, 10$.

$\lambda = 1.25$ and $\epsilon = 0.3$. For $t > \lambda\tau$, $f(g, t)/n(1, t)$ achieves steady state.

different from Eq. 2 does not change the scaling form of Eq. 14 even though the value of λ will be different. This will be discussed in detail later.

Equation 14 is obtained under the condition of $\partial n(1, t)/\partial t = 0$. In fact, this condition can be relaxed. It is clear from Eq. 10 that Eq. 14 is valid as long as:

$$\left| \frac{\partial f(x, t)}{\partial t} - \frac{\partial n(1, t)}{\partial t} \right| \gg \left| \frac{\partial n(1, t)}{\partial t}, \right|$$

which is obviously satisfied until $\partial f(g, t)/n(1, t)/\partial t = 0$. Subsequently, the dynamic effect of the monomer depletion has to be considered. If the time scale for the depletion of the monomer

$$t_{n1}^{-1} = -\frac{\partial \ln n(1,t)}{\partial t}, \tag{16}$$

is taken as a time-averaged quantity, Eq. 10 with Eqs. 4 and 5 can be solved to obtain the CSD in the NBL as:

$$\frac{f(g, t)}{n(1, t)} = \frac{1}{\sqrt{\pi}} \exp\left[-\frac{W(g)}{kT} \right] \exp\left(\frac{\lambda\tau}{t_{n1}}\right) \times \int_{X + \exp[-(t-\lambda\tau)/\tau]}^{X + \exp(\lambda)} \frac{e^{-z^2} dz}{(z - X)^{\tau/t_{n1}}}. \tag{17}$$

As expected, for $t_{n1} \gg \tau$, Eq. 17 reduces exactly to Eq. 14. For $t \gg \lambda\tau$ and $t_{n1} \gg \tau$, Eqs. 17 and 14 reduce to:

$$\frac{f(g, t)}{n(1, t)} = \frac{1}{2} \exp[-W(g)/kT] \operatorname{erfc}\left[\frac{g - g_*}{\delta} \right] \tag{18}$$

which is the CSD about g_* when the time scale for the depletion of monomer is larger than the nucleation time scale, τ.

The condition $t_{n1} \gg \tau$ implies that:

$$n(1, t)/n(1, 0) \gg \exp(-t/\tau), \tag{19}$$

for nucleation in solids without requiring long-range transport, and

$$n(1, t)/n(1, 0) \gg \frac{1}{1 + t/\tau_o} \tag{20}$$

for the general case of $n_c(t) = n(1, t)$, where $\tau_o = \tau(t = 0)$. Both Eqs. 19 and 20 can be satisfied, $t_{n1} \gg \tau$, before the complete depletion of the nucleation sites.

Consequently, Eq. 14 is valid only before the complete depletion of the monomer. Moreover, since cluster-cluster interactions such as coagulation are not considered in Eq. 1, Eq. 14 should also be limited to the precoalescence stages. Therefore, Eq. 14 is valid only in the early stages of nucleation, that is, before the complete depletion of the monomer and the occurrence of coalescence. Equation 17 should be used, instead of Eq. 14, when the effect of the monomer depletion becomes important in some special situations.

Dynamic Scaling of the CSD Beyond the NBL: the Precoalescence Stages

As noted above, the question of how to treat the CSD for sizes beyond the NBL, that is, for supercritical clusters, has defied rigorous analytic solution from early attempts up to the present. No results for the CSD have been obtained previously for $g \gg g_*$ by *directly* solving Eq. 1.

Kinetic description

Equation 1 can be rewritten as:

$$\tau \frac{\partial f(x, t)}{\partial t} = \frac{\epsilon^2 x^{2/3}}{2} \frac{\partial^2 f(x, t)}{\partial x^2} + \left[\frac{x^{-1/3}}{3} \epsilon^2 - 3x^{1/3}(x^{1/3} - 1) \right] \frac{\partial f(x, t)}{\partial x} - x^{-1/3}(2 - x^{-1/3}) f. \tag{21}$$

For sizes beyond the NBL, the terms containing ϵ^2 in Eq. 21 can no longer be allowed to be discarded simply because $3kT/W(g_*) = \epsilon^2 \ll 1$.

In the early stages of nucleation before the complete depletion of the nucleation sites and coalescence, the continuing growth of the nucleated clusters is by the addition of monomers, consequently, $f(g, t)$, for $g > g_*$, is a decaying function of g. Following this observation, one can conclude:

$$\left| \frac{\partial^2 f(x, t)}{\partial x^2} \right| \ll \left| \frac{\partial f(x, t)}{\partial x} \right| \tag{22}$$

Consequently, for $g > g_*$, it is possible to discard the term containing the second derivative of f in Eq. 21. In comparison with the other term containing $\partial f(x, t)/\partial x$, it is also possible to discard the term $(x^{-1/3}/3)\epsilon^2 \partial f(x, t)/\partial x$. Thus, the reduced kinetic equation valid for sizes beyond the NBL is:

$$\tau \frac{\partial f(x, t)}{\partial t} = -3x^{1/3}(x^{1/3} - 1) \frac{\partial f}{\partial x} - [x^{-1/3}(2 - x^{-1/3})] f. \tag{23}$$

Equation 23 can be solved if the necessary boundary condition is known.

Since $f(g, t)$ in the NBL given by Eq. 13 is valid for $t > 0$

and is asymptotically valid at $g_o/g_* \approx 1+1.1\epsilon$ (Shi and Seinfeld, 1992), hence, the necessary boundary condition given by:

$$\frac{f(g_o, t)}{n(g_o, t)} = \frac{1}{2}\text{erfc}\left[1.1+\exp\left(-\frac{t-\lambda\tau}{\tau}\right)\right] - \frac{1}{2}\text{erfc}[1.1+\exp(\lambda)]. \quad (24)$$

and the initial condition is given by Eq. 4.

CSD beyond the NBL: precoalescence stages

Since $n(g, t)$ is physically meaningless for $g > g_o$, one cannot introduce $f(g, t)/n(g, t)$ into Eq. 23 for $g > g_o$. Instead, one can introduce $y(x, t) = f(x, t)/n(g_o, t)$ into Eq. 23. Solving Eq. 23 with Eq. 24, we obtain the CSD for $g > g_o$:

$$\frac{f(x, t)}{n(x_o, t)} = \frac{1}{2}\left(\frac{x}{x_o}\right)^{-1/3}\left(\frac{x_o^{1/3}-1}{x^{1/3}-1}\right) \times \left\{\text{erfc}\left[1.1+\exp\left(-\frac{t-t_f(g)}{\tau}\right)\right] - \text{erfc}\left[1.1+\exp\left(\frac{t_f(g)}{\tau}\right)\right]\right\}. \quad (25)$$

where

$$t_f(g) = \lambda\tau + t_{\text{growth}}(g_o, g)$$

$$t_{\text{growth}}(g_o, g) \equiv \int_{g_o}^{g}\frac{dg}{\dot{g}_m} = \tau\left[x^{1/3} - x_o^{1/3} + \ln\frac{x^{1/3}-1}{x_o^{1/3}-1}\right]. \quad (26)$$

Here, $t_{\text{growth}}(g_o, g)$ is the time for a cluster to grow from g_o to g, determined by $\dot{g}_m$ that is included in Eq. 1. Comparing Eq. 25 with Eq. 14, it is clear that $f(g, t)/n(1, t)$ for sizes beyond the NBL increases to its steady value following the same time dependence as $f(g, t)/n(1, t)$ for sizes within the NBL does, but with a time shift, t_{growth}.

Equation 25 represents the first result reported for the cluster-size distribution valid at $g > g_o$ in the precoalescence stages of nucleation. By using $g_o/g_* = 1+1.1\epsilon$, the scaling relation presented by Eq. 25 can be made clearer as shown below.

Dynamic scaling

Since the CSD represented by $f(g, t)$ is, in fact, the number concentration at g, $f(r, t)$ can be conveniently obtained from $f(g, t)$ by using $r \propto g^{1/3}$. Here, r is the radius of a g-sized cluster that is taken as spherical. In addition, $x_o \approx 1+1.1\epsilon$, Eq. 25 then can be simplified, for $t > 0$, as:

$$f(r, t) = n(1, t)\phi[t/t(r)]\eta(r), \quad (27)$$

$$\eta(r) \approx \sqrt{\frac{kT}{W_*}}\exp\left(-\frac{W_*}{kT}\right)\left(\frac{r}{r_*}\right)^{-2}\left(1-\frac{r_*}{r}\right)^{-1}$$

$$\phi[t/t(r)] = \text{erfc}\left[1.1+\exp\left(-\frac{t-t_f(r)}{\tau}\right)\right] - \text{erfc}\left(1.1+\exp\left(\frac{t_f(r)}{\tau}\right)\right]$$

where $r/r_* = (g/g_*)^{1/3}$ and $t_f(r) = t_f[g(r)]$:

$$\frac{t_f(r)}{\tau} \approx \frac{r}{r_*} + \ln\left(\frac{r}{r_*}-1\right) - 2 + \ln\frac{3W_*}{kT} \quad (28)$$

Therefore, a dynamic scaling relation has been predicted for the CSD:

$$\frac{f(r, t)}{n(1, t)\phi[t/t(r)]} = \eta(r). \quad (29)$$

For $r \gg r_o > r_*$,

$$\eta(r) = \sqrt{\frac{kT}{W_*}}\exp\left(-\frac{W_*}{kT}\right)\left(\frac{r}{r_*}\right)^{-2} \sim r^{-2} \quad (30)$$

The dynamic scaling for $f(g, t)/n(1, t)$ for $g > g_o$ is sketched in Figure 3.

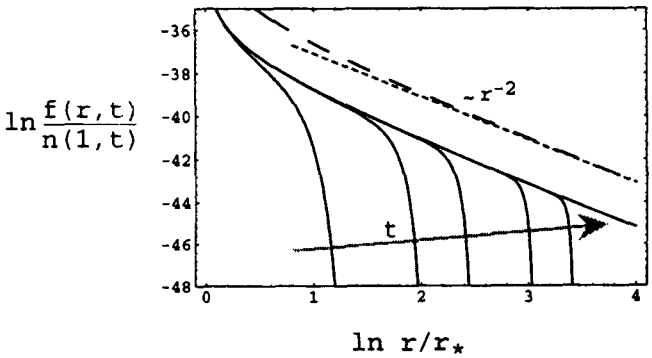

Figure 3. Dynamic evolution of the CSD for sizes beyond the NBL in the precoalescence stages of nucleation and growth according to Eq. 29.

Power-law distribution

As shown in Figure 3, at each given $t > 0$ in the precoalescence stages of nucleation and growth, there is a size range, $r_o < r < r_m(t/t_f)$ in which

$$f(r, t)/n(1, t) \propto r^{-2} \quad (31)$$

where $r_m(t/t_f)$ is a cutoff size. For $r < r_m(t/t_f)$, $f(r, t)/n(1, t)$ achieves time independence. A plot of $\ln f(r, t)$ vs. $\ln r$ at a given $t > 0$ is then a straight line with a slope of -2.

The same asymptotic power law behavior of the CSD will be obtained if Eq. 17 is a boundary condition at $g = g_o$ for solving Eq. 23 for $g > g_o$.

The results obtained can be extended to nucleation of clusters of any dimension, d, with

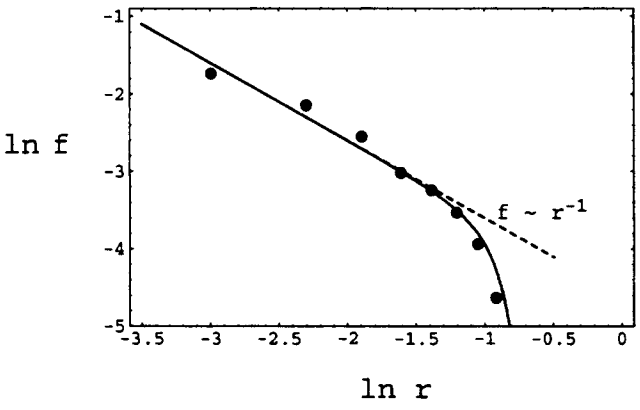

Figure 4. Grain-size distribution from an isothermally annealed Si thin-film for 10 h at $T=608°C$.

The size range is from $r=0.05$ to 0.4 μm (Kumomi et al., 1991). The points display experimental measurements of $f(r, t)$. The units for f are μm^{-2}. The solid curve represents the prediction based on Eq. 29. The dashed straight line indicates a power law with the exponent of -1.

$$\beta(g) \propto g^{(d-\nu)/d}, \quad W(g) = -g\Delta\mu + s\sigma g^{(d-1)/d}. \tag{32}$$

Then, for $t>0$ and sizes beyond the NBL, the CSD obeys:

$$f(r, t)/n(1, t) \propto r^{-(d-\nu)}. \tag{33}$$

Therefore, in general, there is a power-law subrange in the spectrum of the cluster-size distribution in the precoalescence stages of nucleation and growth, the exponent of which depends only on the interphase monomer transfer mechanism contained in $\beta(g)$. In general, the average cluster shape and $\beta(g)$ change with time; therefore, the exponents are expected to vary with time too.

Discussion

The deterministic growth rate is the difference between the rate of addition and that of dissociation (Christian, 1975):

$$\dot{g} \equiv dg/dt = \beta(g, t)\left[1 - \exp\left(\frac{\partial}{\partial g}\frac{W(g)}{kT}\right)\right]. \tag{34}$$

However, the deterministic growth rate implied by Eq. 1, $\dot{g}_m$, is consistent with Eq. 34 only for $\partial W/\partial g < kT$. In this sense, Eq. 1 is valid in the region near the NBL where the condition $\partial W/\partial g < kT$ can be satisfied. Using Eq. 34, Eq. 1 can be generalized naturally as:

$$\frac{\partial f(g, t)}{\partial t} = \frac{\partial}{\partial g}\left[\beta(g)\frac{\partial f(g, t)}{\partial g} - \dot{g} f(g, t)\right] \tag{35}$$

where $\dot{g}$ is given by Eq. 34 or other similar expressions corresponding to different growth mechanisms.

Even though a particular functional form of $W(g)/kT$, that is, Eq. 2, is used in deriving $f(r, t)/n(1, t)$, a change in the functional form of $W(g)/kT$ does not change the scaling forms and their asymptotic limits for $f(r, t)/n(1, t)$ and others. The reason for the universality is that $W(g, t)/kT$ determines only the magnitudes of $\mu(g)$, λ and $t_{\text{growth}}(g_o, g)$, and does not influence the dependence of $f(r, t)/n(1, t)$ on r as has been shown above.

Asymptotic power-law CSDs are frequently associated with nonequilibrium phenomena (Domb and Green, 1972; Mandelbrot, 1982). The discovery of the asymptotic power-law CSD in the early stages of nucleation and growth is, to our knowledge, reported here for the first time. A preliminary analysis of the data (Kumomi et al., 1991) from an amorphous Si thin film isothermally annealed at 608°C supports the power-law prediction. The results of this analysis are displayed in Figure 4. Figure 4 shows that there is a well-defined size range $0.05\ \mu m < r < 0.25\ \mu m$, in which the grain-size distribution obeys $f \propto r^{-1}$, as predicted by this work. The solid curve in Figure 4 presents the prediction of the CSD from Eq. 29, which agrees with the measurement. It is clear that the overall picture predicted for the evolution of the cluster-size distribution at the nucleation and growth stages has been confirmed.

Other Scaling Behavior of Nucleation Beyond the NBL in the Precoalescence Stages

For sizes beyond the NBL, the cluster flux and the accumulated cluster number density can be readily obtained from Eq. 25.

Dynamic scaling of cluster flux

For sizes beyond the NBL, $g>g_o$, $J(g, t)$ can be obtained from $f(g, t)$ given by Eq. 25 as:

$$\frac{J(r, t)}{J_{so}(g_*)}\frac{n(1, 0)n_c(0)}{n(1, t)n_c(t)} = \frac{1}{\text{erfc}(1.1)}\left\{\text{erfc}\left[1.1 + \exp\left(-\frac{t-t_f}{\tau}\right)\right] - \text{erfc}\left[1.1 + \exp\left(\frac{t_f}{\tau}\right)\right]\right\}, \tag{36}$$

Equation 36 shows that the scaled cluster flux reaches its steady value by following the same time dependence as the scaled CSD, Eq. 25. Equation 36, however, does not follow the same time dependence as the cluster flux about g_* which can be obtained from Eq. 14. Therefore, the commonly used assumption that the time dependence of the cluster flux for sizes beyond the NBL is the same as that within the NBL is incorrect. For $r_o \ll r < r_m(t/t_f)$, one has from Eq. 36 that:

$$\frac{J(r, t)}{J_{so}(g_*)} = \frac{n(1, t)n_c(t)}{n(1, 0)n_c(0)}. \tag{37}$$

Accumulated cluster number density measured at sizes beyond the NBL

First, it should be noted that the relations obtained previously for the accumulated cluster number density measured in the supercritical size range usually do not consider the time variation of $n(1, t)$. For example, in our previous work (Shi and Seinfeld, 1991, 1992), the following two relations were obtained:

$$\frac{N(g \geq g_d, t)}{J_{so}(g_*)\tau} = E_1(e^{-[(t-t_f)/\tau]}) - E_1(e^{t_f/\tau}), \quad t \gg t_f(g) \tag{38}$$

and

$$N(g \geq g_d, t) = J_{so}(g_*)[t - \tau_e(g)], \quad t \gg t_f(g) \tag{39}$$

$$\tau_e(g) = 0.5772\tau + t_f + \tau E_1(e^{t_f/\tau}), \quad t_f = t_f + 0.7885\tau$$

Equation 39 indicates that for $t \gg t_f$, $N(g, t)$ becomes linear with t; however, Eqs. 38 and 39 are incorrect for both small and large time limits. In the limit of small times, $t < t_f$, our previous result for $f(g, t)$ (Shi et al., 1990, 1991) had a discontinuity problem at $t = 0$. In the limit of large times, no consideration was given to the time change of $n(1, t)$.

The actual accumulated cluster number density measured at $g_d > g_o$ in the presence of the depletion of $n(1, t)$ can be obtained by using $J(r_d, t)$ given by Eq. 36:

$$N(g \geq g_d, t) = \int_0^t J(g_d, t')dt'. \tag{40}$$

That is,

$$\frac{N(r \geq r_d, t)}{J_{so}(g_*)} = \frac{1}{n(1, 0)n_c(0)\text{erfc}(1.1)} \int_0^t n(1, t')n_c(t') \times \left\{ \text{erfc}\left[1.1 + \exp\left(-\frac{t' - t_f(r_d)}{\tau} \right) \right] - \text{erfc}\left[1.1 + \exp\left(\frac{t_f(r_d)}{\tau} \right) \right] \right\} dt'. \tag{41}$$

In contrast to Eq. 38 or 39, Eq. 41 predicts that for $t \gg t_f(r_d)$,

$$\frac{N(r \geq r_d, t)n(1, 0)n_c(0)}{\int_0^t n(1, t')n_c(t')dt} = J_{so}(g_*). \tag{42}$$

which provides another simple means to obtain the steady-state rate of nucleation, $J_{so}(g_*)$. As can be seen from Eq. 41, $N(g, t)$ becomes time invariant for $t \gg t_f(r_d)$, that is expected physically before the complete depletion of the monomer.

General Foundation for Nucleation Kinetic Measurements

The CSD in the precoalescence stages of nucleation is the most important measurement to evaluate the mechanism of nucleation and provides a definite test of the microscopic models involved in nucleation theories, including $W(g)$ and $\beta(g)$. An outline is presented of a direct and straightforward approach to obtain experimentally the nucleation barrier and its temperature dependency by measuring the CSD for sizes beyond the NBL in the precoalescence stages of nucleation and growth.

In principle, Eq. 14 can be applied to data obtained in the NBL and its vicinity, that is, in the nanometer or subnanometer size range. It, however, is frequently possible to obtain accurately the CSD for sizes beyond the critical one, in the micron or submicron size range. Thus, Eq. 25 provides an essential means of determining W_*/kT as shown below.

One can rewrite Eq. 25 for $f(r, t)$ in the power-law subrange, $r_o < r < r_m(t/t_f)$, as:

$$\ln\frac{f(r, t)}{n(1, t)} = -(d - \nu)\ln\frac{r}{r_1} - \frac{W_*}{kT} + \ln\left[\text{erfc}(1.1)\left(\frac{r_*}{r_1}\right)^{(d-\nu)} \sqrt{\frac{6.8kT}{d(d-1)W_*}} \right]. \tag{43}$$

The above universal relationship between $f(r, t)/n(1, t)$ and W_*/kT allows one to determine W_*/kT by measuring the CSD for sizes beyond the NBL in the precoalescence stages of nucleation and growth, since the exact value of r_*/r_1 does not affect greatly the estimated value of W_*/kT. Applying Eq. 43 to the data presented in Figure 4 and for r_*/r_1 ranging from 1 to 10, the estimated W_*/kT changes from about 25 to 28. Taking the average of 25 and 28, W_*/kT is found to be about 26.5, 2.1 eV. $n(1, 0)$ is estimated as $8K/a^3$, where a is the lattice constant and K is the film thickness.

Once the activation energy of nucleation for a specific problem has been determined, Eq. 42 can be used to determine β_* and its temperature dependency.

Conclusions

Systematic approaches have been developed to obtain the cluster-size distribution, $f(r, t)$, for sizes within the nucleation barrier layout and beyond. We have shown that the cluster-size distribution within and beyond the NBL in the early stages of nucleation obeys universal scaling relations. In a range of sizes beyond the nucleation barrier layer, $f(r, t)$ exhibits a universal power-law distribution, the exponent of which depends only on the monomer addition mechanism. The cluster flux, $J(g, t)$, also exhibits a dynamic scaling relation. The dynamic scaling relations established for the cluster-size distribution and other kinetic laws of nucleation are universal, since they depend on $W(g)/kT$, but not its particular form. A preliminary comparison with an experimental study confirms the predicted dynamic scaling and the power-law behavior of the cluster-size distribution for $g > g_o$ in the early stages of nucleation and growth. The universal kinetic laws of nucleation establish a general foundation for nucleation kinetic measurements including the determination of the nucleation barrier and the interfacial monomer transport rate by measuring the cluster-size distribution in the precoalescence stages of nucleation and growth.

Acknowledgment

We would like to express our appreciation to Hideya Kumoni for providing the data used in Figure 4, as well as for his many comments that are indispensable in resolving several issues presented in this article, in particular the issue of the discontinuity at $t = 0$ associated with the solution for the transient cluster-size distribution obtained in an early work (Shi et al., 1990).

Notation

d = effective dimensionality of the cluster

dg/dt = average cluster growth rate
$\mathrm{erfc}(x)$ = complementary error function
$E_1(x)$ = exponential function
$f(g, t)$ = cluster number density at g and time t
g = number of monomers in a cluster
g_* = number of monomers in the critical size cluster
$\bar{g}_m$ = average cluster growth rate
g_o = number of monomers in the nucleated cluster
$J(g, t)$ = cluster flux
$J_s(g_*, t)$ = $n(1, t)\beta(g_*)Z$
J_{so} = $J(g_*, t=0)$
k = Boltzmann constant
$n(g, t)$ = equilibrium cluster number density
$n(1, t)$ = monomer density
$n(1, 0)$ = $n(1, t=0)$
$n_c(t)$ = monomer concentration around clusters
$N(g, t)$ = accumulated cluster number density
r = cluster radius
r_* = radius of the critical cluster
s = geometric constant
t = time
$t_f(g)$ = characteristic time for $f(g, t)/n(1, t)$ to reach steady state for $g > g_o$
$t_{n1}(g)$ = characteristic time for the relative time variation of $n(1, t)$
T = temperature
$W(g)$ = cluster formation energy
W_* = $W(g_*)$
x = g/g_*
x_o = g_o/g_*
X = $(x-1)/\epsilon$
y = $f(x, t)/n(x, t)$
Z = Zeldovich factor

Greek letters

$\beta(g, t)$ = monomer addition rate to a g-sized cluster
β_* = $\beta(g_*, t)$
γ = Euler's constant
δ = half width of the nucleation boundary layer
$\Delta\mu$ = nucleation driving force
ϵ = δ/g_*
$\eta(r)$ = dimensionless function
θ = dimensionless surface energy
$\lambda\tau$ = characteristic time for $f(g, t)/n(1, t)$ to reach its steady state in the nucleation boundary layer
ν = index for different modes of monomer addition
τ = characteristic time for a cluster to cross the nucleation boundary layer
τ_o = $\tau(t=0)$
$\phi(r)$ = dimensionless function

Literature Cited

Bender, C. M., and S. A. Orszag, *Advanced Mathematical Methods for Scientists and Engineers*, McGraw-Hill, New York (1978).

Christian, J. W., *The Theory of Transformations in Media and Alloys*, Pergamon, Oxford (1975).

Domb, C., and M. S. Green, eds., *Phase Transition and Critical Phenomena*, Vol. 1, Academic, New York (1972).

Feder, J., K. C. Russell, J. Lothe, and G. M. Pound, "Homogeneous Nucleation and Growth of Droplets in Vapors," *Adv. Phys.*, **5**, 111 (1966).

Frenkel, J. I., *Kinetic Theory of Liquids*, Clarendon, London (1946).

Kelton, K. F., "Crystal Nucleation in Liquids and Glasses," *Solid State Phys.*, **45**, 75 (1992).

Kumomi, H., T. Yonehara, and T. Noma, "Manipulation of Nucleation Sites in Solid-State Si Crystallization," *Appl. Phys. Lett.*, **59**, 3565 (1991).

Mandelbrot, B. B., *The Fractal Geometry of Nature*, Freeman, San Francisco (1982).

Mon, K. K., and D. Jasnow, "Finite Size Scaling and Critical Nucleation," *Phys. Rev. Lett.*, **59**, 2983 (1987).

Russell, K. C., "Nucleation in Solids: The Induction and Steady State Effects," *Adv. Coll. Interf. Sci.*, **13**, 205 (1980).

Shi, F. G., and J. H. Seinfeld, "Transient Kinetics of Nucleation," *Nucleation and Atmospheric Aerosols*, p. 1, N. Fukuta and P. Wagner, eds., Deepak Publ., Hampton (1992).

Shi, G., J. H. Seinfeld, and K. Okuyama, "Transient Kinetics of Nucleation," *Phys. Rev. A*, **41**, 2101 (1990).

Shi, G., J. H. Seinfeld, and K. Okuyama, "Reply to a Comment," *Phys. Rev. A*, **44**, 8443 (1991).

Shi, G., and J. H. Seinfeld, "Kinetics of Binary Nucleation: Multiple Pathways and the Approach to Stationarity," *J. Chem. Phys.*, **93**, 9033 (1990).

Shi, G., and J. H. Seinfeld, "Transient Kinetics of Nucleation and Crystallization: I," *J. Materials Res.*, **6**, 2097 (1991).

Shi, G., J. H. Seinfeld, and K. Okuyama, "Homogeneous Nucleation in Spatially Inhomogeneous Systems," *J. Appl. Phys.*, **68**, 4550 (1990).

Shi, F. G., and J. H. Seinfeld, "Nucleation in the Pre-coalescence Stages: Universal Kinetic Laws," *Materials Chem. and Phys.*, in press (1993).

Tu, K. N., J. W. Mayer, and L. C. Feldman, *Electronic Thin Film Science*, Macmillan, New York (1992).

Zettlemoyer, A. C., ed., *Nucleation*, R. Decker, New York (1969).

Manuscript received Mar. 22, 1993, and revision received June 9, 1993.